

Preparation and thermal stability of nickel nanowires via self-assembly process under magnetic field

HU WANG, MING LI, XIAOYU LI, KENAN XIE and LI LIAO*

School of Chemical Engineering, Sichuan University, Chengdu 610065, People's Republic of China

MS received 26 January 2015; accepted 7 May 2015

Abstract. Nickel nanowires were synthesized via a template-free method in an aqueous solution system combined with chemical reduction and magnetic field. The suitable concentration of Ni ions and reaction time were controlled in order to obtain nickel wires with uniform sizes. The products were characterized by X-ray diffraction, scanning electron microscopy, transmission electron microscopy, thermogravimetry and differential scanning calorimetry. The results showed that the Ni nanowires with large aspect ratio up to 200 had uniform size and morphology, about 200 nm. Especially, it is noteworthy that the samples were stable in air when the temperature was lower than 318°C. The study would provide a facile method to prepare nickel nanowires with homogeneous diameter and high thermal stability, which could be used in catalysing CO₂ hydrogenation.

Keywords. Nickel nanowires; magnetic field; self-assembly; thermal stability.

1. Introduction

In recent years, catalytic hydrogenation of CO₂ to light hydrocarbon has been recognized as one of the most effective and economical ways to fix and utilize a large amount of anthropogenic CO₂ and plays a key role in the energy field.^{1–3} Nickel is considered as efficient hydrogenation catalyst both in the conversion and selectivity of CO₂ hydrogenation, which has been extensively applied in industry.⁴ Nanoparticles of metals possess the advantages of small grain diameter and high-specific surface area;⁵ however, the active region on the surface cannot be exposed because of aggregation of the particles.^{6,7} In contrast, one-dimensional nanostructures especially nanowires of metallic materials have much advantages of more active region and more abundant interspaces owing to their unique morphology with a space grid structure. Therefore, it is of great significance to prepare nickel nanowires by an effective method.

Numerous synthesis methods of iron group nanowires have been developed to prepare nanoscale magnetic metal materials.⁸ The approaches of nanowires preparation can be divided into two broad categories: vapour-phase techniques and liquid- or solution-based techniques. The vapour-phase techniques mainly include methods such as chemical vapour deposition (CVD) using catalyst metals, reactive vapour transport, carbothermal reduction, thermal evaporation and thermal decomposition but it remains the disadvantages of high cost and complicated

equipments. Liquid- or solution-based techniques have great industrial application prospect, which include approaches such as sol-gel synthesis, hydrothermal processes and electrodeposition.⁹ Many liquid-phase techniques utilize templates for producing one-dimensional materials. The methods with templates have notable advantages, from which highly ordered and size-controlled nanowires can be obtained.¹⁰ However, the template methods require several steps, including fabrication and removal of templates in order to obtain bare nanowires, which hinders its large-scale applications.^{11–13}

Therefore, it is of great significance and necessity to develop a practical approach to fabricate nanowires, which has the advantages over other methods and have lower temperature, lower cost, less hazardous, simpler equipments, higher yield and more uniform nanowires.¹⁴ Much attention had been paid to the effect of a magnetic field on the nucleation and growth process of magnetic materials and on the self-assembly behaviour of magnetic nanocrystals.^{15–17} It has been indeed found that the magnetic field can significantly influence the movement of magnetic particles.¹⁸ It is, therefore, significant to study the growth and self-assembly behaviour of magnetic nanocrystals under an external magnetic field.

In this paper, a template-free method by combining chemical reduction and magnetic field was applied to prepare nickel nanowires. The properties of prepared nickel nanowires were investigated. Nickel particles were prepared in the absence of a magnetic field to better illustrate the structure directing role of the magnetic field. In order to control the morphology of nickel nanowires, the growth behaviour of nickel was studied. It is possible that

*Author for correspondence (liaolis@scu.edu.cn)

the reduction rate of Ni(II) ions affects the morphology of nickel nanowires.

2. Experimental

2.1 Materials and methods

In the experiments, all the reagents were analytical grade and used as received. The reaction solutions were prepared using nickel sulphate hexahydrate ($\text{NiSO}_4 \cdot 6\text{H}_2\text{O}$) as a source of Ni(II) ions, deionized water as a solvent, hydrazine monohydrate ($\text{N}_2\text{H}_4 \cdot \text{H}_2\text{O}$) as a reducing agent and sodium hypophosphite monohydrate ($\text{NaH}_2\text{PO}_2 \cdot \text{H}_2\text{O}$) as an initiator. Sodium hydroxide (NaOH) was added as a source of OH^- ions. Trisodium citrate dihydrate ($\text{C}_6\text{H}_5\text{Na}_3\text{O}_7 \cdot 2\text{H}_2\text{O}$) was used as a complexing agent and a nucleating agent.

For the synthesis of nickel wires, the reaction solution was kept at 65°C in a water bath, where two parallel neodymium magnets ($60 \times 30 \text{ mm}$) were located inside. The magnetic field intensity was about 15 mT, which is measured by a Tesla meter. In a typical experiment, 0.1 g $\text{NiSO}_4 \cdot 6\text{H}_2\text{O}$, 0.12 g $\text{C}_6\text{H}_5\text{Na}_3\text{O}_7 \cdot 2\text{H}_2\text{O}$ and 60 ml deionized water were mixed in a teflon beaker. A grass-green colour transparent solution was observed after strongly stirring for half an hour. Then 0.25 g NaOH was added in the solution after the mixture was heated to 65°C . After that 2 ml hydrazine monohydrate solution (80 wt%) and 0.01 g $\text{NaH}_2\text{PO}_2 \cdot \text{H}_2\text{O}$ were added into the solution, and the colour changed from grass green to sky blue. After

several minutes, nickel wires were washed three times with deionized water and ethanol. The final products were dispersed in ethanol or dried in a vacuum oven at 50°C for 24 h.

2.2 Characterization

The size and morphology of the products were characterized on a field-emission scanning electron microscope (FESEM, JHOL, S-450). The composition and crystallographic properties of the products were analysed by X-ray diffraction (XRD, Philips, X'pert) in the range from 20° to 90° . Transmission electron microscopy (TEM), high-resolution TEM (HRTEM) images and selected area electron diffraction (SAED) patterns were obtained by a JEOL JEM-100CX TEM. The Ni samples were heated from 30 to 800°C at a rate of $10^\circ\text{C min}^{-1}$ by a thermogravimetric (TG) analyser and differential scanning calorimeter (DSC) (NETZSCH STA 449C) in air atmosphere to study its thermostability.

3. Results and discussion

3.1 Self-assembly process and preparation of nickel nanowires

Figure 1 shows the SEM images of nickel particles and wires synthesized from the solutions under a magnetic field at different times.

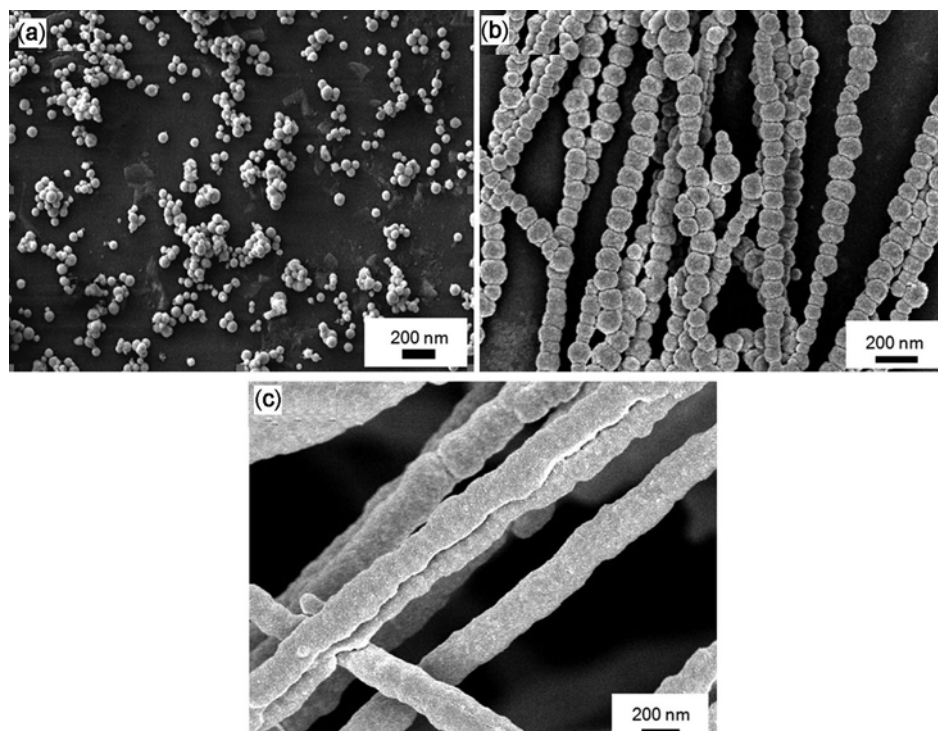


Figure 1. SEM micrographs of products prepared after reaction proceeded (a) 10 min, (b) 20 min and (c) 30 min.

Figure 1a shows the surface morphology of nanoparticles prepared after a tiny amount of initiators were added in the solution 10 min later. Only single spherical nanoparticle with an average particle size of 80 nm can be observed, which can be inferred that the external magnetic field did not play an obvious directing role on the formation of the nanoparticles when the particle size was less than a critical value.

Figure 1b shows the nickel nanochains after the reaction was proceeded 20 min. Single nanoparticles began to be arranged along a straight line under the magnetic field and single dispersed particles were disappeared in the visual field. The average particle size was about 150 nm, which illustrated the fact that the particle diameter was continuously increased when the reaction proceeded.

Figure 1c shows the SEM photograph of nickel nanowires prepared after reacting for 30 min, and the linear nanowires were formed instead of bead chain. Nickel ions in the solution were then reduced on the surface of the prepared nickel nanochains due to the autocatalysis of nickel, which led to the increase of diameter and better linearity of nickel nanowires. And the surface of prepared nickel nanowires was relatively smoother than nickel nanochains.

Figure 2 presents the difference in morphology between the eventual products prepared with (a) and without (b) an external magnetic field applied during particle's growth. The morphology of (b) appears disorderly, consisting of single nearly spherical nanoparticles, while (a) contains highly oriented straight wires; it indicates that a magnetic field can effectively affect the aggregation of nickel nanocrystals. When no external magnetic field is applied, the orientation of each magnetic domain is spontaneously random. The nanocrystals may magnetize one another by dipolar interaction in an arbitrary direction, which cannot finally result in the formation of nanowires. The XRD patterns of the products prepared with and without an external magnetic field applied are similar, which suggested that the external magnetic field affect the morphology of nickel nanowires merely.

To verify the formation mechanism of nickel wires under an external magnetic field various parallel experiments were carried out. The regular patterns can be inferred that the length and diameter had an increasing trend with the extension of reaction time, as shown in figure 3. When the reaction proceeded slowly, spherical particles would have enough time to grow in a larger size. As a result, the growth trend along the direction of magnetic field was restrained in some degree, which led to a short-length and chain-like nickel wires. On the other hand, it may be tough to control the morphology to be linear and uniform with an excessively fast reaction rate. However, the actual aggregating process is very complicated, determined by nucleation, spacial hindrance, magnetic attraction of excessive finer particles and other kinetic factors. When the reaction rate was appropriately

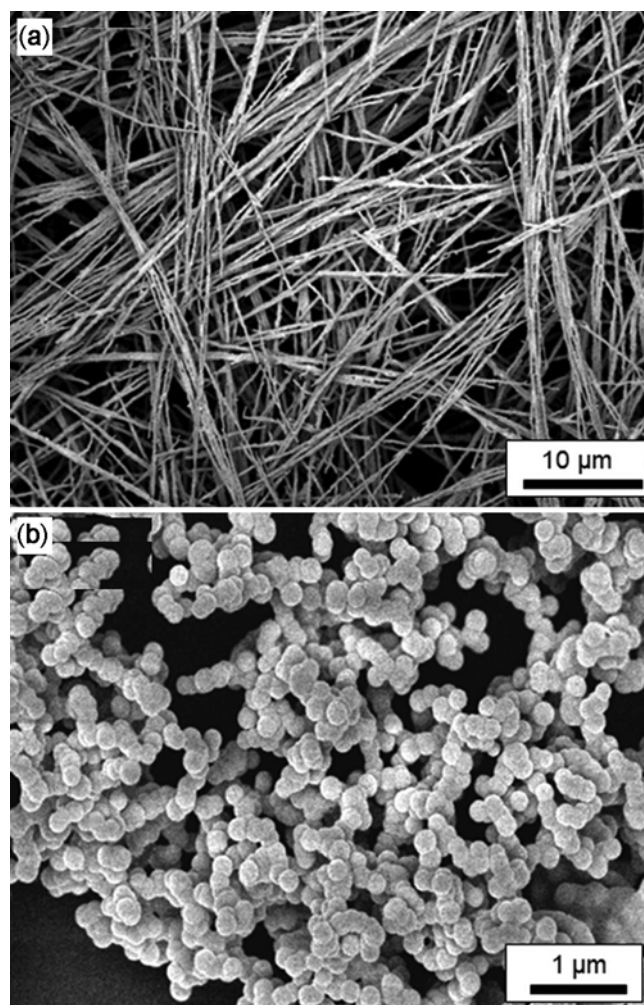


Figure 2. SEM micrographs of products prepared (a) with and (b) without an external magnetic field.

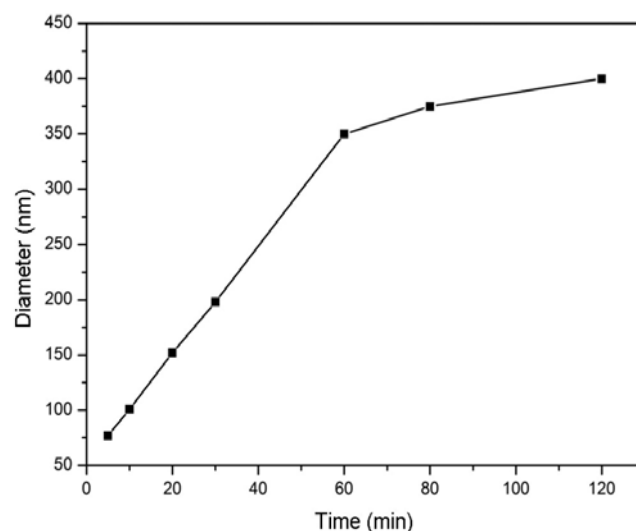


Figure 3. Relationship of the reaction time and particle diameter.

controlled, acicular nickel nanowires with diameter from 200 to 500 nm can be prepared.

3.2 XRD, TEM with SAED of nickel nanowires

Figure 4 shows the corresponding XRD spectrum for the resultant wires. It can be well indexed with the reflections of face-centred cubic Ni (PDF standard cards, JCPDS 04-0850, space group Fm-3m), without impurity peaks. Three characteristic peaks ($2\theta = 44.46^\circ$, 51.81° and 76.49°) corresponding to Miller indices (111), (200) and (220), respectively, were observed. The cell parameter was $a = 3.524$ nm, $b = 3.524$ nm and $c = 3.524$ nm. The average crystalline grain size of linear powders was 20.7 nm, calculated from the XRD patterns according to the Scherrer formula: $L = \lambda k / \cos \beta \theta$. It was obviously smaller than the size of the particles in FESEM micrograph, which implied that one particle was consisted of several crystalline grains.

Figure 5 exhibits typical TEM image of the nickel nanowires and the SAED pattern. It can be seen that nickel particles are assembled well to solid linear structure under the magnetic field. The SAED pattern is composed of several diffraction rings, indicating the polycrystalline property, and the corresponding crystal face is marked on the photograph.

3.3 Thermal stability of nickel nanowires

It is essential to study the stability of the nickel nanowires in air atmosphere considering its application in hydrogenation. The prepared nanowires were characterized by using TG analyser and DSC. As shown in figure 6, between 30 and 318.0°C , there was a little weight loss which may be caused by the evaporation of remained liquid in the samples, nickel nanowires began to oxidize

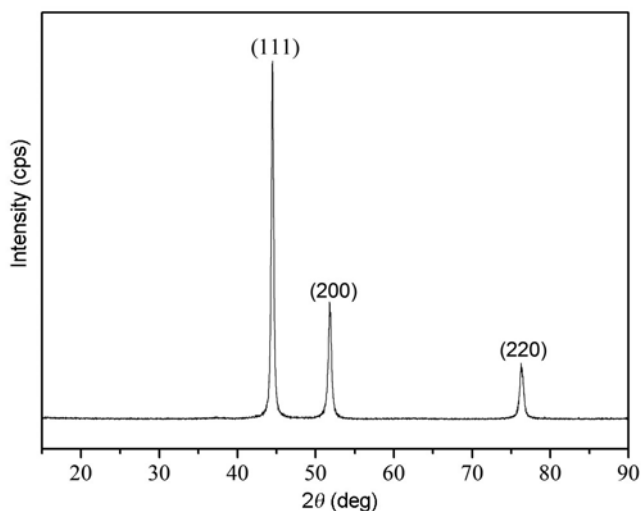


Figure 4. XRD pattern of nickel nanowires.

at 318.0°C and the oxidation rate approaches to maximum at 447.4°C . The final weight gain is about 22.55% which is different with the theoretical weight gain (27.3%) for perfect conversion of pure Ni to NiO. This datum indicates that the oxidation process from Ni to NiO is not complete yet at about 900°C . The DSC curve declines and an exothermic peak appears at 882.1°C , it may be caused by the crystal transformation of nickel at 882.1°C . And it can be inferred that the nickel wires fabricated via the liquid phase method without template are thermally stable in air below 318°C , which would largely expand its application.

To further analyse the stability of nickel nanowires under air atmosphere, nickel nanowires were annealed in air at various temperatures. Figure 7 shows XRD patterns of nickel nanowires annealed at different temperatures. Compared with XRD pattern at room temperature, characteristic peaks of NiO appeared at 300°C , which illustrated that the sample had been oxidized. When the annealing temperature rose to 500°C , NiO occupied a

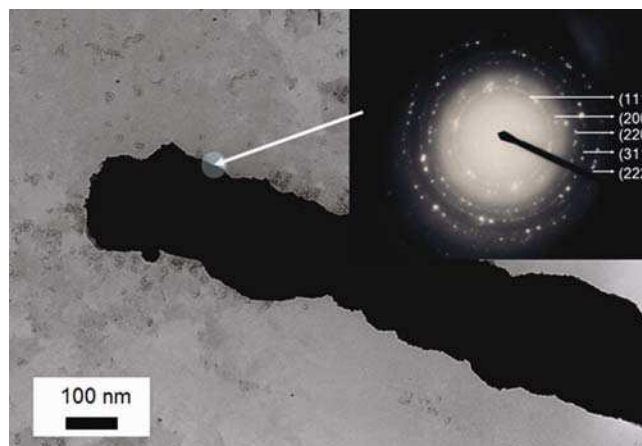


Figure 5. TEM image of nickel nanowires with selected area electron diffraction (SAED) pattern.

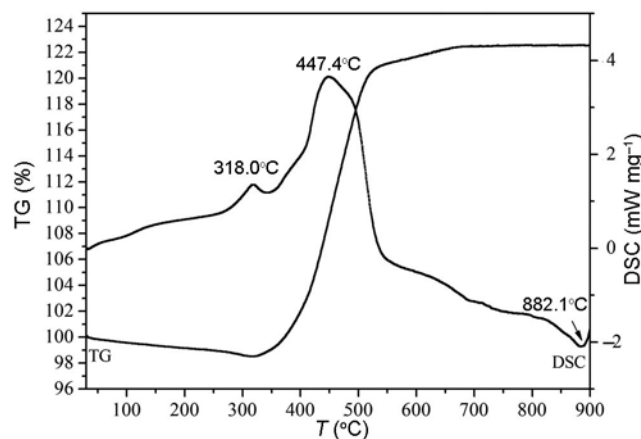


Figure 6. TG/DSC analysis of nickel nanowires.

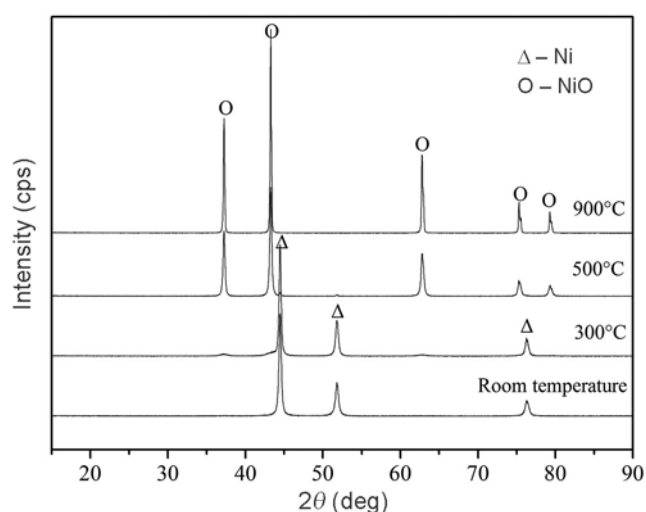


Figure 7. XRD patterns of prepared nickel nanowires annealed in air atmosphere at various temperatures.

strong majority in the annealed samples; meanwhile, hardly the characteristic peaks of Ni can be found. As the annealing temperature rose to 900°C, Ni was totally oxidized to NiO. However, it cannot be easily jumped to the conclusion that there is no transformation to NiO in air atmosphere above 500°C just on account of the similar XRD patterns from 500 to 900°C. An interesting phenomenon was discovered that the colour was diverse at different annealing temperatures, which indicated the existence of chemical transformation in the process. Light grey, bottle green colour appeared, corresponding to 500 and 900°C, respectively. Cubic NiO (PDF standard cards, JCPDS 47-1049, space group $Fm\bar{3}m$) and hexagonal NiO (PDF standard cards, JCPDS 44-1159, space group $R\bar{3}m$) coexisted from 500 to 900°C and the characteristic peaks of them was too close to be distinguished. Hexagonal NiO decreases with the rising of temperature and cubic NiO increases, from which it can be inferred that cubic NiO is more stable and appears green. To sum up, the colour change of NiO may be caused by the crystal transformation.

4. Conclusions

Polycrystal nickel nanowires with an average diameter of about 200 nm were successfully prepared by a template-free method combined chemical reduction and magnetic field. It is found that an external magnetic field can make acicular nickel wires one-dimensionally self-assembled with their magnetic easy axes aligned along the magnetic line of force, leading to the formation of polycrystal nanowires. Nickel particles aggregated larger spherical

particles rather than nickel nanowires in the absence of a magnetic field. In the present work, it can be inferred that the rate of reaction played a crucial role on the morphology of nickel nanowires. When the reaction proceeded excessively slow or rapid, acicular nickel nanowires with relatively low diameter and long length can hardly be obtained. Nickel nanowires are stable in air when the temperature is lower than 318°C. The present study provides a facile method to prepare nickel nanowires with homogeneous diameter in a large scale, which would broad their practical applications.

Acknowledgements

Financial supports by the National Natural Science Foundation of China (Grant no. 50904046) are gratefully acknowledged.

References

1. Janke C, Duyar M S, Hoskins M and Farrauto R 2014 *Appl. Catal. B: Environ.* **152–153** 184
2. Tao X M, Wang J M, Li Z W and Ye Q G 2013 *Comput. Theor. Chem.* **59** 1023
3. Sathawong R, Koizumi N, Song C S and Prasassarakich P 2013 *J. CO₂ Utiliz.* **3** 102
4. Tang S C, Zheng Z, Vongehr S and Meng X K 2011 *J. Nanopart. Res.* **13** 7085
5. Karim S and Maaz K 2011 *Mater. Chem. Phys.* **130** 1103
6. Zhang H J and Liu Y 2008 *J. Alloys Compd.* **458** 588
7. Lin S W, Chang S C, Liu R S, Hu S F and Jan N T 2004 *J. Magn. Mater.* **282** 28
8. Chen D L and Gao L 2005 *Chem. Phys. Lett.* **405** 159
9. Han S, Chen H Y, Chen C C and Yuan T N 2007 *Mater. Lett.* **61** 1105
10. Garcia C, Lecante P, Neumeier D and Verelst M 2008 *Mater. Lett.* **62** 2106
11. Rahman Z, Razeeb M, Rahman A and Kamruzzaman D 2003 *J. Magn. Mater.* **262** 166
12. Huang D, Zhang Q and Qiao P Z 2011 *Comput. Mater. Sci.* **50** 903
13. Byrne F, Mello P, Whelan A and Davies A 2009 *J. Magn. Mater.* **321** 1341
14. Shi J B, Chen Y C, Lee C W, Wu C and Chen C J 2008 *Mater. Lett.* **62** 2218
15. Peng C X, Gong J H and Wang L 2009 *Comput. Mater. Sci.* **16** 229
16. Hellenthal C, Ahmed W, Kooij S and Silfhout V 2012 *J. Nanopart. Res.* **14** 1107
17. Moustafa F and Daoush M 2007 *J. Mater. Process. Technol.* **181** 59
18. Chen H Y, Xu C J, Zhou X, Liu Y Q and Zhao G Z 2012 *Mater. Res. Bull.* **47** 4353